# SYNTHESIS OF COPPER (II) COMPLEXES WITH ANTITUMOR ACTIVITY

By

Michael Alan Baird

A capstone project submitted for
Graduation with University Honors

February 16, 2017

University Honors
University of California, Riverside

APPROVED

_____
Dr. Jack Eichler
Department of Chemistry

_____
Dr. Richard Cardullo, Howard H Hays Jr. Chair and Faculty Director, University Honors
Associate Vice Provost, Undergraduate Education

Abstract

Glioblastoma is the most commonly occurring brain cancer, with over 100,000 new cases per year, worldwide. There is no known cure for glioblastoma and the median survival time after diagnosis is between twelve and fifteen months. Chemotherapeutics such as Cisplatin (cisdiamminedichloroplatinum(II)) have numerous side effects, motivating research for drugs based on other transition metals, including copper (II). The results of Inci et al indicated that bis polypyridyl copper (II) complexes may have enhanced cytotoxicity over mono complexes. In an effort to expand the library of Copper(II) based anticancer drugs, bis complexes containing bipyridine (bipy) derivatives as ligands have been synthesized and characterized. All synthesis reactions were completed by adding appropriate equivalents of each ligand to a copper(II) ion. $[(4,4'\text{ dimethylbipy})_2Cu](NO_3)_2$ and $[(6,6'\text{ dimethylbipy})_2Cu](NO_3)_2$ were successfully made by reacting $Cu(NO_3)_2*2.5H_2O$ with two equivalents of the appropriate ligand in methanol at $50^oC$. These characterizations are supported by X-ray crystallography and elemental analysis, which indicate that a pure product was formed for both reactions. $[(6,6'\text{ dimethylbipy})_2Cu]Cl_2$ was made by reacting $[(6,6'\text{dimethylbipy})Cu]Cl_2$ with $AgBF_4$ and one equivalent of 6,6'dimethylbipy in acetonitrile at $50^oC$. $[(4,4'\text{ dimethylbipy})ClCu(\mu\text{-}Cl)_2CuCl(4,4'\text{ dimethylbipy})]$ was made by reacting $(4,4'\text{ dimethylbipy})CuCl_2$ and 4,4' dimethylbipy in acetonitrile at $50^oC$. These compounds are likewise confirmed by X-ray crystallography, although elemental analysis indicates impurity. The presence of an additional ligand on the reported bis complexes was predicted to stabilize the interaction between the complex and DNA, potentially enhancing the cytotoxicity of these bis complexes compared to their mono counterparts. Sulforhodamine B (SRB) assays with

GL261 glioblastoma cells showed that one of the bis complexes, $[(4,4'\text{dimethylbipy})_2Cu](NO_3)_2$, inhibited cell growth better than its corresponding mono complex. $[(6,6'\text{dimethylbipy})_2Cu](NO_3)_2$, on the other hand, did not inhibit cell growth better than its corresponding mono complex. My hypothesis that the bis copper (II) complexes would inhibit cell growth better than their mono counterparts was not necessarily true for the complexes we made and/or for the cancer we chose to study. Future work will test the redox stability and quantitative DNA binding of these copper complexes.

Acknowledgements

I would like to thank the following individuals for their contributions: Dr. Jack Eichler, for teaching me the basics of inorganic synthesis, holding me accountable to work diligently, and sharing his passion for research; Dr. Fook Tham, for determining the x-ray crystal structures of my compounds; Dr. Emma Wilson, Noah Angel, Raneen Khatib, Justin Rubalcava, Jocelyn Rodriguez, and Isaac Kehinde, for their contributions and support.

I thank the UC Riverside Department of Chemistry and UC Riverside Student Mini-Grant program for their generous funding.

Contents

Tables and Figures

# 1. Introduction

## 1.1 Glioblastoma

Glioblastoma is the most common form of brain cancer and one of the deadliest, with a median survival time between 12-15 months and a 5 year relative survival rate less than 5% [1]. Although the most common age to become diagnosed with glioblastoma is 65-74, it regularly effects children and teenagers. There is no known cure or prevention method for this cancer that kills over 60,000 people each year[2]. In an effort to find a drug that can effectively treat glioblastoma with limited side effects, I have synthesized four new compounds and tested two them for *in vitro* efficacy in inhibiting glioblastoma growth.

Glioblastoma is a cancer of astrocytes, star shaped cells that form the connective tissue in the brain and regulate osmosis in neurons. Glioblastoma tumors are often diffuse through large areas of the brain and have branches that extend the the tumor into healthy tissue[3]. The unique structure of these cancers makes surgical removal difficult, so surgery is often followed by chemotherapy and radiation therapy[4]. Chemotherapy is generally preferred to radiotherapy when children are being treated due to the developmental effects associated with radiotherapy.

Temozolomide is a standard chemotherapeutic used for treatment of glioblastoma. Although it can slow down cancer growth, it is not regarded a cure[5]. Furthermore, some patients are resistant to this DNA methylating agent, as its cytotoxic effects can be negated by MGMT, a DNA repair protein that is often overexpressed in cancer patients[6]. Temozolomide has evident shortcomings, stimulating research in medicinal chemistry. Clearly, there is a need for glioblastoma drugs that are selective, powerful, and effective in small dosages.

## 1.2 Metal-based Chemotherapies

Much of the ongoing going research in cancer chemotherapeutics has involved coordination complexes, a class of molecules defined as a metal atom covalently bonded to at least one nonmetal ion or neutral molecule, known as a ligand. These compounds usually involve the d-orbitals of the metal, allowing for interesting geometries and electronic properties. The metal center, characterized by its electron count and redox activity, anchors the molecule, while the ligands, often large organic molecules, form a structural framework that contribute to the function of the complex. With applications in electronics, gas storage, and fuel cells, coordination complexes are a frequently studied class of molecules in chemistry and materials science.

While many scientists have utilized coordination complexes for their physical properties, complexes are vital in biological systems. Hemoglobin, for example, contains a protein-iron(II) complex that transports oxygen in the bloodstream. Coordination chemistry is essential to human life. In addition to their biochemical usefulness, the structure and straightforward syntheses of organometallic complexes give them great advantages in drug development. One common coordination complex as a pharmaceutical is Auranofin, a gold(I) molecule that functions as an anti-inflammatory and is used to treat rheumatoid arthritis and leukemia[7]. Recent research in medicinal inorganic chemistry has been particularly focused on cancer because of the developing research in oncology and the discovery of cancer-inhibiting platinum complexes.

### 1.2.1 Platinum Drugs

First approved for treatment of testicular and ovarian cancer in 1978, Cisplatin (cisdiamminedichloroplatinum(II)) is one of the most commonly prescribed antitumor drugs. Patients diagnosed with many different types of cancers have been treated and/or cured through cisplatin treatment[8]. Cisplatin is driven to enter cancer cells through diffusion, as cancer cells are often deficient in chloride[9]. Once it enters the cell, cisplatin undergoes an aquation reaction, releasing a chloride ion to restore equilibrium. The aquated complex is thought to cause cell death by intrastrand adduction of DNA, the formation of multiple coordination bonds with nitrogen atoms in the nitrogenous bases. Formation of these adducts is not correctable by DNA repair proteins. DNA is prevented from participating in necessary cell processes and cell death ensues. Cisplatin is generally regarded as the principal treatment method for ovarian, testicular, and bladder cancers.[10] Despite its widespread use, this platinum(II) coordination complex is notorious for its side effects including nausea, renal toxicity, decreased blood cell production, and even loss of hearing. Additionally, some patients develop a resistance to cisplatin[11].

Polynuclear platinum complexes have been investigated for anticancer properties, including a BBR3464, a complex that contains 3 platinum atoms. The mechanism of these polynuclear platinum complexes is similar to cisplatin, with the additional possibility of cell death by interstrand adduction[9]. Although BBR3464 showed higher cytotoxicity than cisplatin and carboplatin in preclinical trials, phase I trials reveal dose-limiting side effects.

In addition to severe side effects, the high cost of platinum adds another motivation to research complexes based on other metals. The shortcomings of cisplatin in treating glioblastoma have driven scientists to study other complexes based on other metals as

chemotherapeutics. Ruthenium, gold, and copper are three metals that have attracted a large part of this interest.

### 1.2.2 Ruthenium Drugs

An interesting advantage of ruthenium is its ability to mimic iron when binding to certain biomolecules[9]. Amin et al explains that proteins that transfer iron into cells are often over expressed in cancer cells. Because of ruthenium's similarity to iron and the overexpression of transferrin receptors, it often accumulates in cancerous tissue. Ruthenium drugs thus have a potential for selectivity.

Complexes of ruthenium in the II and III oxidation state have shown promising results. They can be attracted to cancerous tissue, and may even become activated to their cytotoxic form by the low oxygen levels in tumors[12]. However, clinical trials for one of the most promising ruthenium drugs, NAMI-A, resulted in adverse side effects, including blister formation on the hands and feet of patients. None of the patients had cancer remission. KP1019, another promising ruthenium drug, caused no side effects[9] in a phase I clinical trial and prevented tumor growth for patients with several kinds of solid cancers[12]. This ruthenium complex causes cell death by activating Capsase-3, which in turn initiates the intrinsic mitochondrial pathway, a biochemical pathway that results in apoptosis. While no ruthenium complexes are clinically approved as chemotherapeutics, they deserve further investigation.

### 1.2.3 Gold Drugs

Gold coordination chemistry is well studied and very diverse. Many researchers studying coordination complexes as chemotherapeutics have been particularly interested in gold (III). This ion is isoelectronic to platinum (II), so complexes of gold (III) were

initially thought to function by a similar mechanism to platinum-based drugs, which adduct DNA and inhibit cell replication, resulting in cell death. However, gold cancer drugs are now thought to inhibit other cellular targets, including thioredoxin reductase and proteostomes[13]. This difference in cellular targets allows some gold drugs to inhibit growth in cell lines that are resistant to cisplatin.

Gold coordination complexes have been synthesized and tested for a range of different diseases. However, with the exception of auranofin, used to treat rheumatoid arthritis and leukemia, most gold complex drugs failed to treat the disease intended and caused an array of side effects[14]. Although some gold complexes have shown promising results in a research setting, no new gold drugs have been clinically approved since auranofin, in 1985.

### 1.2.4 Copper drugs

A common link between complexes of platinum, gold, and ruthenium, is that they all involve a metal that has no natural biochemical role. The side effects associated with these drugs may arise from this; because they do not occur naturally in the body, they are unable to be safely metabolized. Furthermore, they each have a very small recommended daily allowance (see figure 1). Copper, on the other hand, has many direct uses in the body as a structural and catalytic cofactor[15]. Most notably, copper is present at the active site of cytochrome C oxidase, the protein that concludes oxidative phosphorylation. Copper has a well-studied role in the human body and has a recommended daily allowance that is much higher than that of platinum, gold, or ruthenium[16]. Copper's natural role in the body gives it a potential advantage of being safely metabolized, reducing side effects.

Copper's potential as a chemotherapeutic goes deeper than just being safe for the human body; its unique interactions with cancer cells give it potential for selective toxicity to cancer cells. Copper salts are known to accumulate in cancerous tissues much more so than other tissues[15]. Other copper-containing materials, such as the protein azurin, have been shown to preferentially enter cancerous cells. This may indicate that other copper containing compounds may be selective to cancer cells.

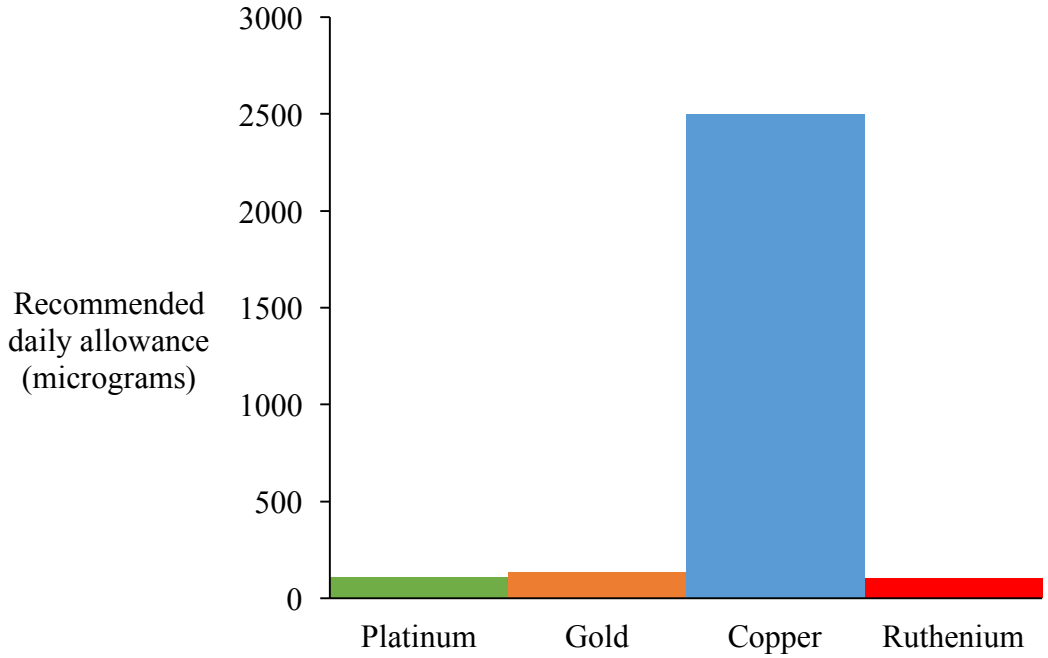


Figure 1: FDA recommended daily allowance of selected metals being researched as chemotherapeutics[16]

Copper has also been shown to be an important cofactor that helps cancer cells to grow[17]. This detail may be seen as reason to prevent copper from entering cancerous cells. However, most efforts to limit cancer growth by chelating copper have not been successful[15]. Rather than preventing copper from entering cancerous cells, the natural attraction for copper to enter cancer cells may be harnessed by attaching a cytotoxic drug to the copper atom. Because copper atoms are more likely to enter to cancerous cells,

cytotoxic drugs that include a copper atom may be selective to cancer cells over other cells. The general theory of the selectivity of copper drugs was shown to be true for very similar complexes to those reported in this paper. Eichler et al showed that Copper (II) bipy drugs selectively inhibited growth in glioblastoma cancer cells over healthy human foreskin fibroblast cells. The observed selectivity of copper compounds means that they are unlikely to affect non-cancerous tissues, potentially reducing side effects.

### 1.3 Mono-polypyridyl Copper Complexes

The potential for copper based anticancer drugs is strengthened by research that has shown their effectiveness against several different cell lines. In fact, Pivetta et. al reports a copper (II) complex with phenanthroline that is 37 times more cytotoxic than Cisplatin against a line of lung cancer cells[18]. The mechanism by which copper complexes kill cancerous cells typically involves DNA adduction and cleavage[18]. Copper complexes involving polypyridyl ligands will often bind to DNA in the minor groove[19], stabilized by pi-pi stacking interactions between the spaced aromatic rings of the ligand and the aromatic rings in the nitrogenous bases[15]. Once the complex is bound to DNA, copper can uniquely catalyze DNA cleavage through phosphate ester hydrolysis and deoxyribose sugar oxidation.

The promising results and distinct biochemical mechanisms of copper (II) mono-polypyridyl drugs make them an excellent candidate as a cancer therapeutics. The potential for less severe side effects makes copper drugs especially advantageous. In summary, copper (II) polypyridyl complexes have selectivity for cancerous cells, unique redox properties, simple synthetic procedures, high affinity for DNA, and are relatively

affordable. Copper complexes may be the solution for defeating dangerous cancers like glioblastoma.

### 1.4 Target Bis-polypyridyl Copper Complexes

Research by Inci et al has shown increased cytotoxicity when polypyridyl copper complexes contain an additional equivalent of a ligand[19]. The presence of an additional polypyridyl ligand may help to stabilize the interactions with DNA. Many other bis complexes have shown increased cytotoxicity over their mono counterpart[15]. This experiment will determine if the bis complexes [Cu(4,4' dimethylbipy)$_2$]$(NO_3)_2$ and [Cu(6,6' dimethylbipy)$_2$]$(NO_3)_2$ inhibit growth in GL261 glioblastoma cells better than their mono counterparts. The synthesis and *in vitro* efficacy of these bis compounds are described herein.

## 2. Methodology

### 2.1 Synthetic procedures

In an effort to expand upon the library of bis polypyridyl copper complexes, the following compounds were synthesized.

#### 2.1.1 Synthesis of Cu(6,6' dimethylbipy)$_2(NO_3)_2$ (Compound **1**)

A methanol solution of 6,6' dimethylbipy (128 mg, 0.695 mmol) was added to a methanol solution of $Cu(NO_3)_2 \cdot 2.5H_2O$ (81 mg, 0.695 mmol). The reaction mixture turned from light blue to Kelly green upon addition of ligand. The reaction mixture stirred for 30 minutes at room temperature. The mixture was then set out for recrystallization by slow evaporation. Some green and orange crystallites formed on the sides of the vial. These were pushed back into the mixture and dissolved, then the vial was placed in a refrigerator. After a week, no crystals were formed, so the liquid was moved using a rotary evaporator, leaving

a green and brown/orange solid. This was washed with cold ether and dried on a Shlenk line. A small amount was submitted for elemental analysis. The remaining solid was split into two parts for recrystallization; one with acetonitrile and one with methanol. Both solvents evaporated off. The remaining solids were dissolved in acetonitrile and combined for recrystallization by slow evaporation. These crystals were submitted for X-ray crystallography analysis.

2.1.2 Synthesis of [Cu(4,4' dimethylbipy)$_2$]($NO_3$)$_2$ (Compound **2**)

Compound 2 was synthesized analogously to compound 1, using 0.188 g of 4,4' dimethylbipy (1.02 mmol) and 0.118 g of $Cu(NO_3)_2 \cdot 2.5H_2O$ (1.02 mmol). When adding the 4,4' dimethylbipy to methanol, not all of the solid transferred, so the actual amount that went into solution was less than 1.02 mmol. This reaction mixture stirred at room temperature for 30 minutes, during which the solution turned from light blue to dark blue. The solution was set out for recrystallization by slow evaporation. A crystalline solid formed and the supernatant was removed and placed in a new vial. The solid was washed with cold ether and dried on a Shlenk line. Some white solid floated in the ether during the wash step. This was assumed to be residual $Cu(NO_3)_2 \cdot 2.5H_2O$ that did not react (since there were incorrect stoichiometric ratios) and thrown out. The crystalline solid was submitted for elemental analysis. The supernatant that was decanted produced more crystals, which were submitted for X-ray crystallography analysis.

2.1.3 Synthesis of Cu(6,6' dimethylbipy)$_2Cl_2$ (Compound **3**)

This procedure was adapted from Eichler et al. $CuCl_2*2H_2O$ (43 mg, 0.25 mmol) was added to a flask and dissolved in acetonitrile. 6,6' dimethylbipy (109 mg, 0.59 mmol) dissolved in acetonitrile was added dropwise to the flask. No color change was observed

at this point. Silver tetrafluoroborate (58 mg, 0.29 mmol) dissolved in acetonitrile was added dropwise to the flask, causing the reaction mixture to turn green. After the mixture stirred for one hour, the mixture was Kelly green. Solvent was removed by rotary evaporation and the remaining solid was redissolved and filtered through celite to remove AgCl. This was put in a refrigerator. After 5 months, crystals formed. These were washed with cold ether, dried on a Shlenk line, and submitted for elemental analysis. The supernatant was placed back in the refrigerator and produced more crystals, which were submitted for X-ray crystallography analysis.

2.1.4 Synthesis of [(4,4' dimethylbipy)ClCu($\mu$-Cl)$_2$CuCl(4,4' dimethylbipy)] (Compound **4)**

40 mg (0.125 mmol) of [Cu(4,4' dimethylbipy)$Cl_2$] and 23 mg (0.125 mmol) of 4,4' dimethylbipy were added to flask and dissolved in acetonitrile. The green mixture turned teal upon mixing. The mixture refluxed at 110°C for 2 hours and was transferred to a beaker for recrystallization by slow evaporation. Blue crystals formed after 3 days. A portion of the crystals were removed, washed with cold ether, and dried on a Shlenk line. This sample was submitted for elemental analysis, while the crystals in the beaker were submitted for X-ray crystallography.

2.2 Elemental Analysis

Elemental analysis is a method of determining the elemental composition of a sample. The sample is combusted in the presence of oxygen and the gaseous products are separated and quantified using gas chromatography[20]. The amount of each gas in the chromatograph is used to calculate the mass of an element in the original sample. If the theoretical composition (determined using the proposed chemical formula) and the actual

composition are similar, then there is a high likelihood that the sample primarily contains the proposed structure. In practice, only the mass percent of carbon and hydrogen are needed to identify the compound. In a combustion reaction, carbon and hydrogen form $CO_2$ and $H_2O$, respectively, which can easily be measured in a gas chromatograph. Elemental analysis for the reported compounds was conducted by Atlantic Microlab, Inc.

## 2.3 X-ray crystallography

### 2.3.1 Compound **1**

A blue-green prism fragment (0.448 x 0.349 x 0.277 $mm^3$) was used for the single crystal x-ray diffraction study of $[C_{24}H_{24}N_4Cu]^{2+}.[NO_3]^-_2.H_2O$ (sample je26_0m). The crystal was coated with paratone oil and mounted on to a cryo-loop glass fiber. X-ray intensity data were collected at 100(2) K on a Bruker APEX2 [24] platform-CCD x-ray diffractometer system (fine focus Mo-radiation, $\lambda$ = 0.71073 Å, 50KV/30mA power). The CCD detector was placed at a distance of 5.0600 cm from the crystal.

A total of 2160 frames were collected for a sphere of reflections (with scan width of 0.5° in $\omega$, starting $\omega$ and 2$\theta$ angles of –30°, and $\phi$ angles of 0°, 90°, 120°, 180°, 240°, and 270° for every 360 frames, 10 sec/frame exposure time). The frames were integrated using the Bruker SAINT software package[25] and using a narrow-frame integration algorithm. Based on a monoclinic crystal system, the integrated frames yielded a total of 58512 reflections at a maximum 2$\theta$ angle of 61.014° (0.70 Å resolution), of which 7633 were independent reflections ($R_{int}$ = 0.0294, $R_{sig}$ = 0.0170, redundancy = 7.7, completeness = 100%) and 6713 (87.9%) reflections were greater than 2$\sigma$(I). The unit cell parameters were, a = 17.7965(7) Å, b = 10.9225(4) Å, c = 12.9657(5) Å, $\beta$ = 97.6389(6)°, V = 2497.94(17) $Å^3$, Z = 4, calculated density $D_c$ = 1.526 g/$cm^3$. Absorption corrections were applied

(absorption coefficient $\mu$ = 0.932 $mm^{-1}$; max/min transmission = 0.782/0.680) to the raw intensity data using the SADABS program[26].

The Bruker SHELXTL software package[27] was used for phase determination and structure refinement. The distribution of intensities ($E^2$-1 = 0.931) and systematic absent reflections indicated one possible space group, P2(1)/c. The space groupP2(1)/c (#14) was later determined to be correct. Direct methods of phase determination followed by two Fourier cycles of refinement led to an electron density map from which most of the non-hydrogen atoms were identified in the asymmetric unit of the unit cell. With subsequent isotropic refinement, all of the non-hydrogen atoms were identified. There was one cation of $[C_{24}H_{24}N_4Cu]^{2+}$, two anions of $[NO_3]^-$, and one molecule of water present in the asymmetric unit of the unit cell.

Atomic coordinates, isotropic and anisotropic displacement parameters of all the non-hydrogen atoms were refined by means of a full matrix least-squares procedure on $F^2$. The H-atoms were included in the refinement in calculated positions riding on the atoms to which they were attached, except the H-atoms of water were refined unrestrained. The refinement converged at R1 = 0.0262, wR2 = 0.0691, with intensity I>2$\sigma$ (I). The largest peak/hole in the final difference map was 0.449/-0.545 e/$Å^3$.

### 2.3.2 Compound **2**

An X-ray structure for this compound was attained, but a procedural write-up is not available due to disorder in the structure. Please see crystallography and elemental analysis results.

2.3.3 Compound **3**

A blue-green prism fragment (0.336 x 0.261 x 0.155 $mm^3$) was used for the single crystal x-ray diffraction study of $C_{24}H_{24}ClN_4Cu.Cl.[CH_3CN].[H_2O]$ (sample je25r_0m). The crystal was coated with paratone oil and mounted on to a cryo-loop glass fiber. X-ray intensity data were collected at 100(2) K on a Bruker APEX2 platform-CCD x-ray diffractometer system (fine focus Mo-radiation, $\lambda$ = 0.71073 Å, 50KV/30mA power). The CCD detector was placed at a distance of 5.0600 cm from the crystal.

A total of 2160 frames were collected for a sphere of reflections (with scan width of 0.5° in $\omega$, starting $\omega$ and 2$\theta$ angles at –30°, and $\phi$ angles of 0°, 90°, 120°, 180°, 240°, and 270° for every 360 frames, 10 sec/frame exposure time). The frames were integrated using the Bruker SAINT software package and using a narrow-frame integration algorithm. Based on an orthorhombic crystal system, the integrated frames yielded a total of 58942 reflections at a maximum 2$\theta$ angle of 61.012° (0.70 Å resolution), of which 4034 were independent reflections ($R_{int}$ = 0.0381, $R_{sig}$ = 0.0148, redundancy = 14.6, completeness = 100%) and 3446 (85.4%) reflections were greater than 2$\sigma$(I). The unit cell parameters were, **a** = 7.7197(3) Å, **b** = 14.3758(6) Å, **c** = 23.3249(10) Å, $\alpha = \beta = \gamma = 90°$, V = 2588.52(18) $Å^3$, Z = 4 calculated density $D_c$ = 1.480 $g/cm^3$. Absorption corrections were applied (absorption coefficient $\mu$ = 1.087 $mm^{-1}$; max/min transmission = 0.850/0.712) to the raw intensity data using the SADABS program.

The Bruker SHELXTL software package was used for phase determination and structure refinement. The distribution of intensities ($E^2$-1 = 1.073) and systematic absent reflections indicated two possible space groups, Pca2(1), and Pbcm. The space group Pbcm (#57) was later determined to be correct. Direct methods of phase determination followed

by two Fourier cycles of refinement led to an electron density map from which most of the non-hydrogen atoms were identified in the asymmetric unit of the unit cell. With subsequent isotropic refinement, all of the non-hydrogen atoms were identified. There were half a molecule of $C_{24}H_{24}ClN_4Cu.Cl$, four half water molecules where two were disordered (each disordered site occupancy factor was 32.4%) and one partially occupied disordered molecule of $CH_3CN$ (disordered site occupancy factor was 17.6%) present in the asymmetric unit of the unit cell. The $C_{24}H_{24}ClN_4Cu$-cation was located at the 2-fold rotation axis parallel to the **a**-axis. The Cl-anion, four water molecules and $CH_3CN$ molecule were located at the mirror plane perpendicular to the **c**-axis.

Atomic coordinates, isotropic and anisotropic displacement parameters of all the non-hydrogen atoms were refined by means of a full matrix least-squares procedure on $F^2$. The H-atoms were included in the refinement in calculated positions riding on the atoms to which they were attached. DFIX commands were used to restrained the H-atoms of all the water molecules. The refinement converged at R1 = 0.0355, wR2 = 0.0953, with intensity, $I>2\sigma(I)$. The largest peak/hole in the final difference map was 0.831/-0.764 e/Å$^3$.

2.3.4 Compound **4**

A blue prism fragment (0.322 x 0.205 x 0.147 mm$^3$) was used for the single crystal x-ray diffraction study of $C_{24}H_{24}N_4Cl_4Cu_2.H_2O$ (sample je23_0m). The crystal was coated with paratone oil and mounted on to a cryo-loop glass fiber. X-ray intensity data were collected at 100(2) K on a Bruker APEX2 platform-CCD x-ray diffractometer system (fine focus Mo-radiation, $\lambda$ = 0.71073 Å, 50KV/30mA power). The CCD detector was placed at a distance of 5.0600 cm from the crystal.

A total of 2160 frames were collected for a sphere of reflections (with scan width

of 0.5° in ω, starting ω and 2θ angles of –30°, and ϕ angles of 0°, 90°, 120°, 180°, 240°, and 270° for every 360 frames, 10 sec/frame exposure time). The frames were integrated using the Bruker SAINT software package and using a narrow-frame integration algorithm. Based on a monoclinic crystal system, the integrated frames yielded a total of 30196 reflections at a maximum 2θ angle of 61.004° (0.70 Å resolution), of which 3888 were independent reflections ($R_{int}$ = 0.0245, $R_{sig}$ = 0.0139, redundancy = 7.8, completeness = 100%) and 3595 (92.5%) reflections were greater than 2σ(I). The unit cell parameters were, **a** = 8.9932(3) Å, **b** = 16.7328(5) Å, **c** = 17.0494(5) Å, **β** = 97.6970(5)°, V = 2542.50(14) Å$^3$, Z = 4, calculated density $D_c$ = 1.712 g/cm$^3$. Absorption corrections were applied (absorption coefficient μ = 2.120 mm$^{-1}$; max/min transmission = 0.746/0.548) to the raw intensity data using the SADABS program

The Bruker SHELXTL software package was used for phase determination and structure refinement. The distribution of intensities ($E^2$-1 = 0.945) and systematic absent reflections indicated two possible space groups, C2/c and Cc. The space group C2/c (#15) was later determined to be correct. Direct methods of phase determination followed by two Fourier cycles of refinement led to an electron density map from which most of the non-hydrogen atoms were identified in the asymmetric unit of the unit cell. With subsequent isotropic refinement, all of the non-hydrogen atoms were identified. There were half a molecule of $C_{24}H_{24}N_4Cl_4Cu_2$ and half a molecule of water present in the asymmetric unit of the unit cell, where both molecules were located at the diagonal glide plane perpendicular to the **c**-axis.

Atomic coordinates, isotropic and anisotropic displacement parameters of all the non-hydrogen atoms were refined by means of a full matrix least-squares procedure on $F^2$.

The H-atoms were included in the refinement in calculated positions riding on the atoms to which they were attached, except the H-atom of water was refined unrestrained. The refinement converged at R1 = 0.0193, wR2 = 0.0506, with intensity I>2σ (I). The largest peak/hole in the final difference map was 0.460/-0.292 e/Å$^3$.

2.4 SRB assay

In order to determine the cytotoxicity of compounds 1 and 2, a Sulfarhodamine B (SRB) assay was conducted. This test determines the extent of cell growth inhibition by comparing the amount of SRB dye uptaken by cell colonies treated with different concentrations of drug. Procedures were adopted from Skehan, et al. GL261 cancer cells were cultured in minimal media supplemented with 10% fetal bovine serum. The cells were diluted and transferred to a 96 well plate so that there were 4000 cells in each well. The plate was incubated overnight at 37 degrees C. After the incubation, compounds 1 and 2 were added in different concentrations from 10-800 nM, along with a negative DMSO control and a positive control of 25 uM $^{\text{sec-butyl}}$phen. The compounds were added in triplicate. The plate was then incubated for 72 hours. The supernatant media in each well was removed and cells were fixed for 1 hour with 10% trichloroacetic acid (100 uL per well). The trichloroacetic acid was removed and the wells were washed 5 times with cold DI water. Then, 50 uL of SRB was added to each well to stain the cells. After a 10 minute incubation period at room temperature, the cells were washed 5 times with 1% trichloroacetic acid. The bound SRB was released by adding 100 uL of unbuffered Tris (pH 10.5). The absorbance at 492 nm were found using a microplate reader. The growth inhibition in wells treated with compounds 1 or 2 was determined directly from the

absorbance of these wells and the negative control using the equation described by Skehan et al.

3. Results and Discussion

All reactions were completed by adding appropriate equivalents of ligands to a copper(II) ion. $[(4,4'\text{dimethylbipy})_2Cu](NO_3)_2$ and $[(6,6'\text{dimethylbipy})_2Cu](NO_3)_2$ were successfully made using a procedure adapted from Inci et al; $Cu(NO_3)_2*2.5H_2O$ was mixed with two equivalents of the appropriate ligand in methanol at 50°C. $[(6,6'\text{dimethylbipy})_2Cu]Cl_2$ was made using a procedure adapted from Eichler et al. $[(6,6'\text{dimethylbipy})Cu]Cl_2$ was mixed with one equivalent of $AgBF_4$ and one equivalent of 6,6'dimethylbipy in acetonitrile at 50°C. [(4,4' dimethylbipy)ClCu(μ-Cl)$_2$CuCl(4,4' dimethylbipy)] was made by reacting (4,4' dimethylbipy)$CuCl_2$ and 4,4' dimethylbipy in acetonitrile at 50°C. Each reaction produced a crystalline solid after a period of slow evaporation. These crystals were used for x-ray crystallography. Remaining crystals were washed with cold ether and dried *in vacuo* for elemental analysis. Each reaction was intended to produce a bis complex. However, reaction 4 yielded a dimer of mono complexes and only reactions 1 and 2 yielded analytically pure products.

Figure 2: Reaction Schemes

Figure 2.1: Reaction **1**

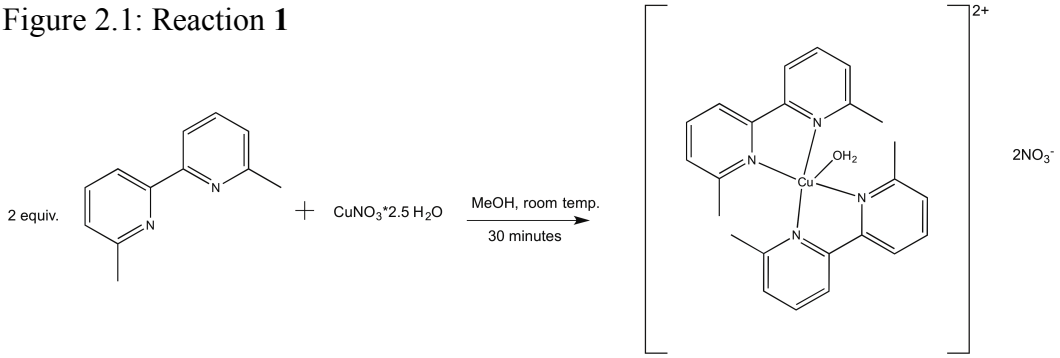


Figure 2.2: Reaction **2**

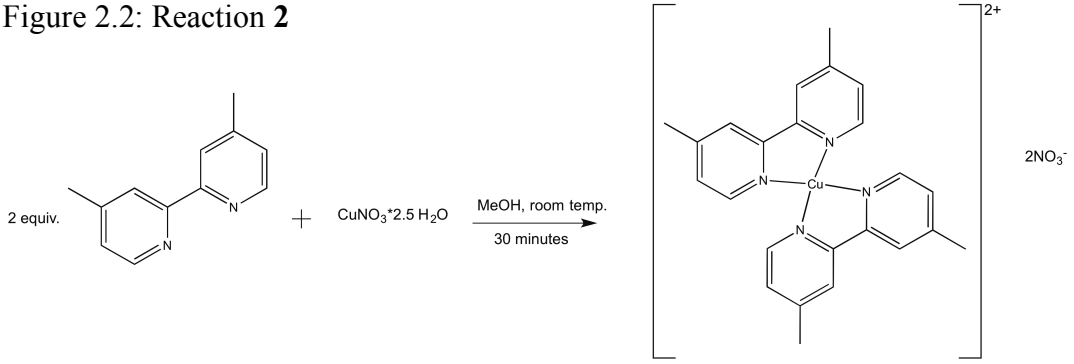


Figure 2.3: Reaction **3**

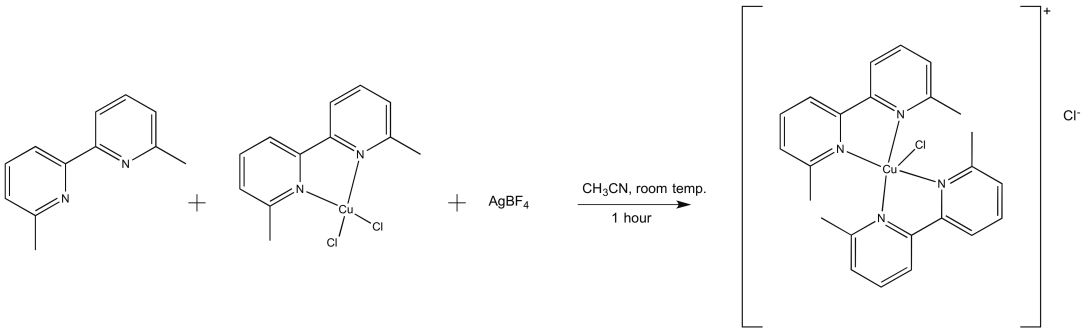


Figure 2.4: Reaction **4**

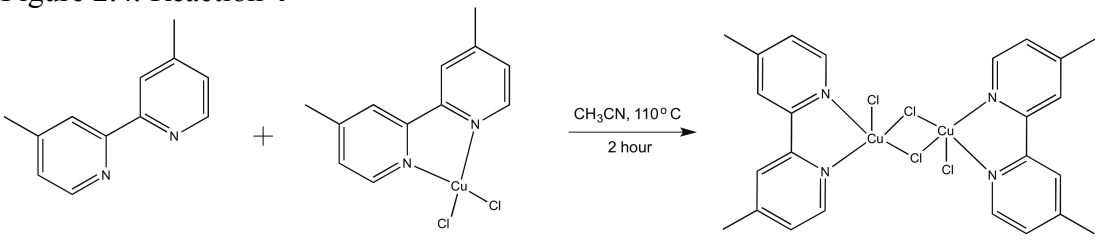

## 3.1 Elemental Analysis

Figure 3: Elemental Analysis Charts

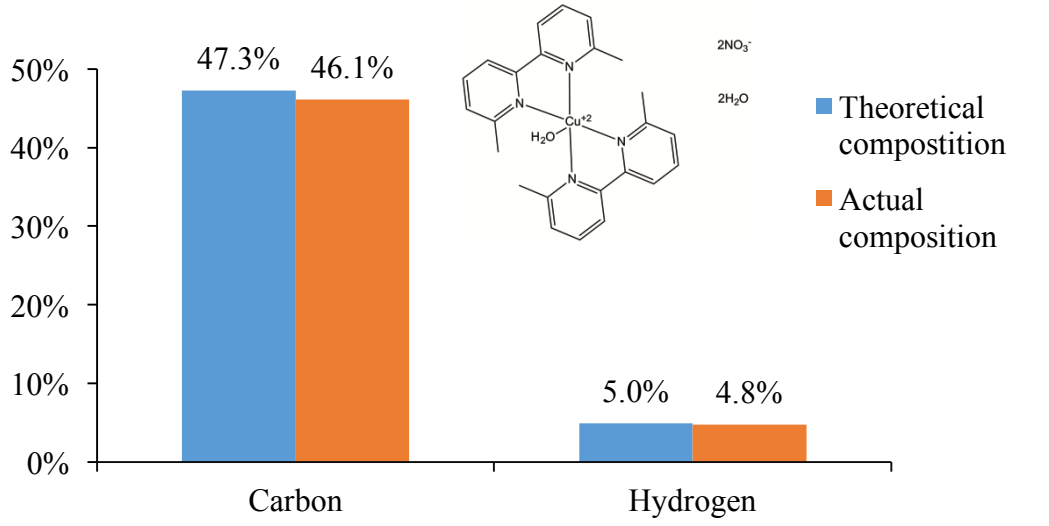


Figure 3.1: Elemental Composition of Compound **1**

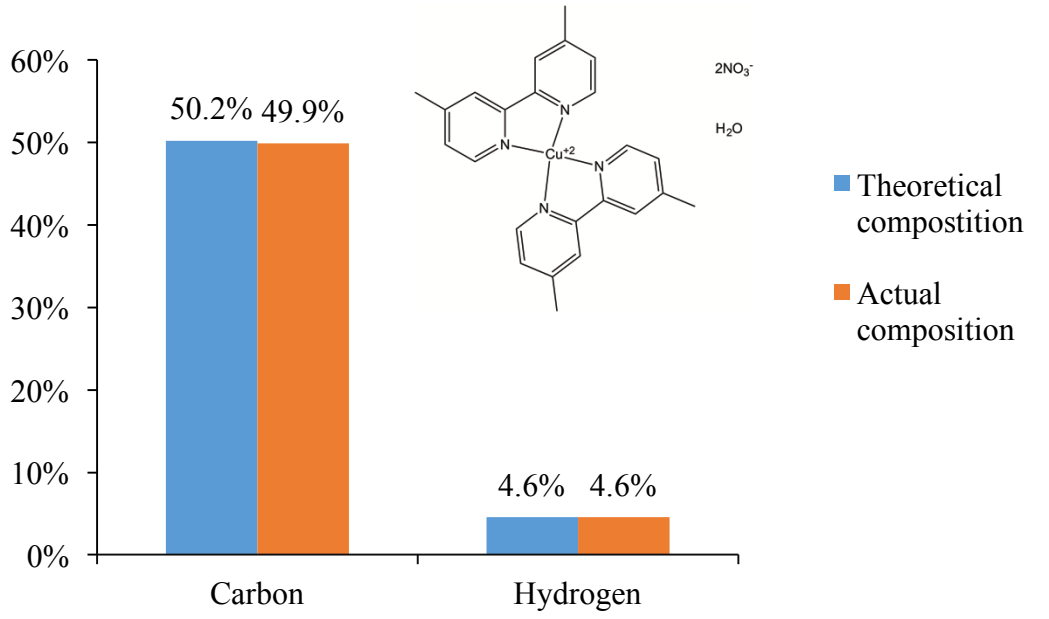


Figure 3.2: Elemental Composition of Compound **2**

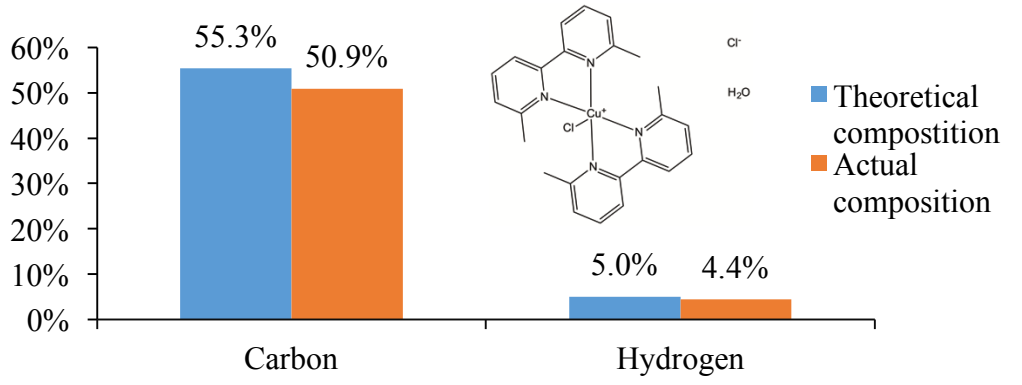


Figure 3.3: Elemental Composition of Compound **3**

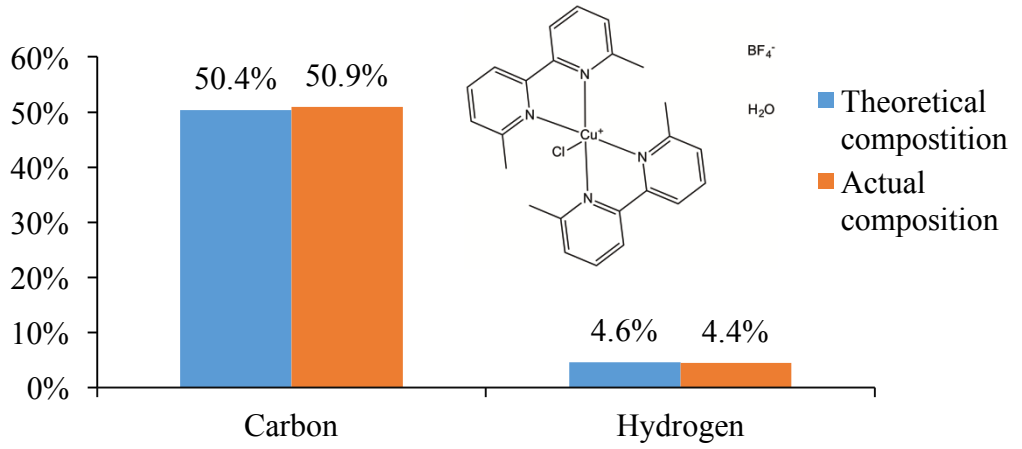


Figure 3.4: Elemental Composition of Compound **3***

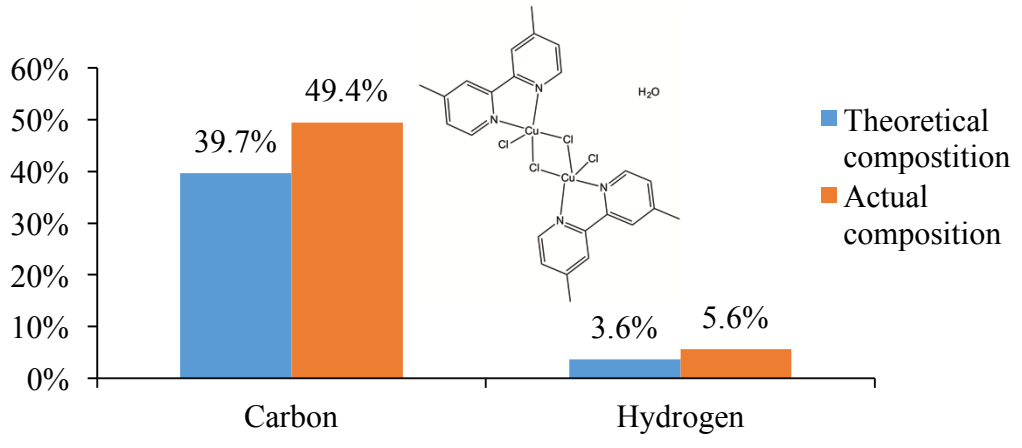


Figure 3.5: Elemental Composition of Compound **4**

The elemental analysis results for compounds 1 and 2 agree very well with the theoretical composition of the product found by x-ray crystallography. The carbon content for compound 1 agrees with the crystal structure within 1.2% and the hydrogen content agrees within 0.2%. The carbon content for compound 2 agrees with the crystal structure within 0.3% and the hydrogen content perfectly agrees with the crystal structure.

For compound 3, the actual composition is very different from the structure found by x-ray crystallography. The x-ray crystal structure shows a bis complex that is covalently bonded to a chloride atom, while a second chloride exists as a counter ion, bonded ionically. The carbon content for compound 3 agrees with the crystal structure within 3.4% and the hydrogen content agrees within 0.6%. This reaction is unique in that it is the only one of the four reactions that involved the reagent silver tetrafluoroborate ($AgBF_4$). This salt was added to the complex to prevent dimer formation by removing one of the two chloride ligands bonded to copper (chloride ligands often function as bridging ligands, as seen in the x-ray structure of compound 4). Removing this ligand would remove steric hindrance and allow the second equivalent of ligand to bond to copper. We hypothesized that the silver ion would displace a chloride ligand and silver chloride would precipitate out of solution. The tetrafluoroborate anion would theoretically balance the positively charged copper complex. Interestingly, the theoretical composition of a bis 6,6' bipy copper complex with one chloride ion and one tetrafluoroborate ion is very close to the actual composition of compound 3 based on elemental analysis. The carbon content for compound 3 agrees with this alternative structure (3*) within 0.5% and the hydrogen content agrees within 0.2%.

This result is unexpected. We observed a cloudy white precipitate in the reaction mixture, which was assumed to be silver chloride. This indicated to us that the reaction went as predicted. Due to misinformation about the reaction, the x-ray crystallography technician may have assumed that the disordered counter ion / solvent mixture in the crystal lattice included a chloride ion instead of a tetrafluoroborate. If this is the case and the structure does actually include a tetrafluoroborate ion, then the elemental analysis results would confirm that the reaction produced an analytically pure [Cu(bis 6,6' dimethylbipy)Cl]$BF_4$. Alternatively, the crystal structure is accurate and the discrepancy in elemental analysis is due to impurity in the product; the similarity of the actual composition to that of [Cu(bis 6,6' dimethylbipy)Cl]$BF_4$ is mere coincidence.

For compound 4, the theoretical composition based on the x-ray crystal structure is very different from the actual composition. The x-ray crystal structure of compound 4 shows a bis complex that is covalently bonded to a chloride atom, while a second chloride exists as a counter ion, bonded ionically. The carbon content for compound 4 agrees differs from the crystal structure by over 10% and the hydrogen content differs by 2%. The carbon and hydrogen content of the actual product is much higher than predicted, indicating that there is an excess of hydrocarbon-like material in the product. This could be due to unreacted polypyridyl ligands, as one molar equivalent of 4,4' bipy was added for each mono copper complex. Theoretically, this did not react and should have been washed away by the cold ether wash. The elemental analysis results indicate that it may have remained. Alternatively, the deviation may be due to ether from the wash that remained in the sample.

## 3.2 X-ray Crystallography

Figure 4: X-ray Crystallography Data

| | Compound 1 | Compound 3 | Compound 4 |
|---|---|---|---|
| Empirical formula | C24 H26 Cu N6 O7 | C24.70 H31.65 Cl2 Cu N4.35 O3.30 | C24 H26 Cl4 Cu2 N4 O |
| Formula weight | 574.05 | 576.74 | 655.37 |
| Temperature | 100(2) K | 100(2) K | 100(2) K |
| Wavelength | 0.71073 Å | 0.71073 Å | 0.71073 Å |
| Crystal system | Monoclinic | Orthorhombic | Monoclinic |
| Space group | P 21/c | P b c m | C 2/c |
| Unit cell dimensions | a = 17.7965(7) Å | a = 7.7197(3) Å | a = 8.9932(3) Å |
| | b = 10.9225(4) Å | b = 14.3758(6) Å | b = 16.7328(5) Å |
| | c = 12.9657(5) Å | c = 23.3249(10) Å | c = 17.0494(5) Å |
| | a= 90°. | a= 90°. | a= 90°. |
| | b= 97.6389(6)°. | b= 90°. | b= 97.6970(5)°. |
| | g = 90°. | g = 90°. | g = 90°. |
| Volume | 2497.94(17) Å3 | 2588.52(18) Å3 | 2542.50(14) Å3 |
| Z | 4 | 4 | |
| Density (calculated) | 1.526 Mg/m3 | 1.480 Mg/m3 | 1.712 Mg/m3 |
| Absorption coefficient | 0.932 mm-1 | 1.087 mm-1 | 2.120 mm-1 |
| F(000) | 1188 | 1199 | 1328 |
| Crystal size | 0.448 x 0.349 x 0.277 mm3 | 0.336 x 0.261 x 0.155 mm3 | 0.322 x 0.205 x 0.147 mm3 |
| Theta range for data collection | 2.193 to 30.507°. | 1.746 to 30.506°. | 2.411 to 30.502°. |
| Index ranges | -25<=h<=25, -15<=k<=15, -18<=l<=18 | -11<=h<=11, -20<=k<=20, -33<=l<=33 | -12<=h<=12, -23<=k<=23, -24<=l<=24 |
| Reflections collected | 58512 | 58942 | 30196 |
| Independent reflections | 7633 [R(int) = 0.0294] | 4034 [R(int) = 0.0381] | 3888 [R(int) = 0.0245] |
| Completeness to theta = 25.242° | 100.00% | 100.00% | 100.00% |
| Absorption correction | Semi-empirical from equivalents | Semi-empirical from equivalents | Semi-empirical from equivalents |
| Refinement method | Full-matrix least-squares on F2 | Full-matrix least-squares on F2 | Full-matrix least-squares on F2 |
| Data / restraints / parameters | 7633 / 0 / 355 | 4034 / 12 / 204 | 3888 / 0 / 164 |
| Goodness-of-fit on F2 | 1.031 | 1.033 | 1.066 |
| Final R indices [I>2sigma(I)] | R1 = 0.0262, wR2 = 0.0691 | R1 = 0.0355, wR2 = 0.0953 | R1 = 0.0193, wR2 = 0.0506 |
| R indices (all data) | R1 = 0.0321, wR2 = 0.0722 | R1 = 0.0427, wR2 = 0.1002 | R1 = 0.0217, wR2 = 0.0519 |
| Extinction coefficient | n/a | n/a | n/a |
| Largest diff. peak and hole | 0.449 and -0.545 e.Å-3 | 0.831 and -0.764 e.Å-3 | 0.460 and -0.292 e.Å-3 |

Figure 5: X-ray Crystal Images

Figure 5.1: X-ray crystal image for compound **1**

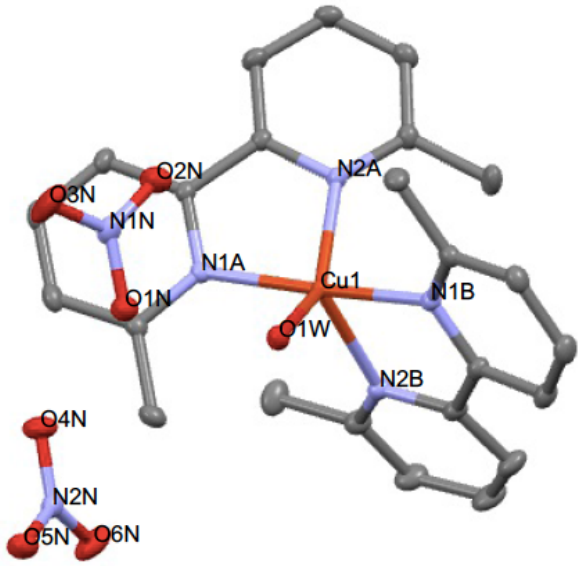


Figure 5.2: X-ray crystal image for compound **2**.
Note disordered counter ion.

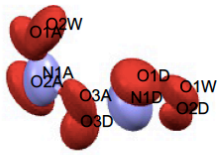


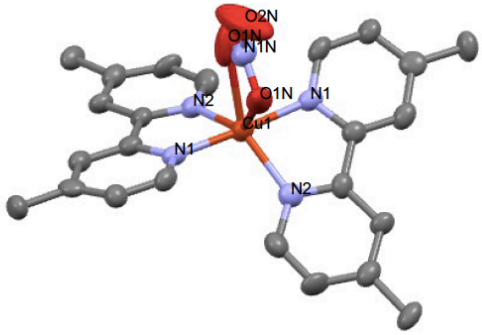

Figure 5.3: X-ray crystal image for compound **3**.
Note disordered solvent/ion cluster.

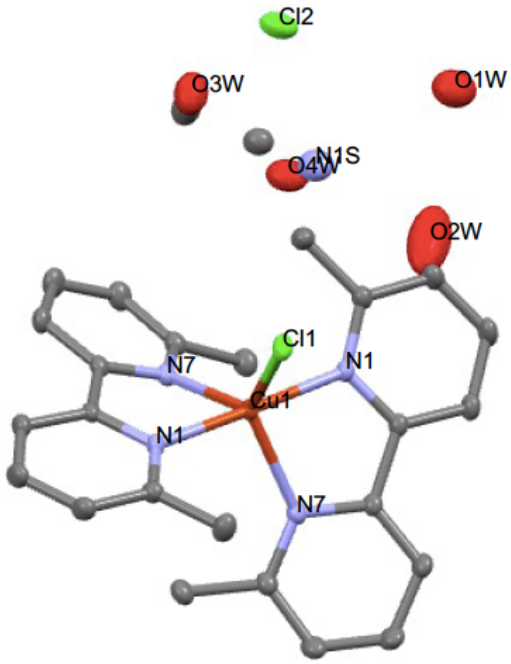


Figure 5.4: X-ray crystal
image for compound **4**

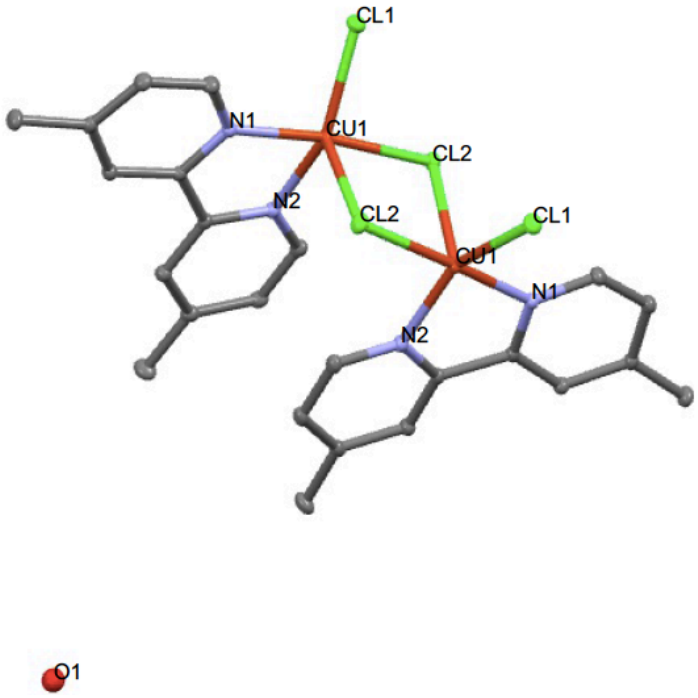

Figure 6: Bond Lengths and Angles from X-ray Crystallography

| Compound 1 | |
|---|---|
| t5=0.43 | |
| Bond length (Angstroms) | |
| Cu(1)-N(1A) | 1.9966(10) |
| Cu(1)-N(1B) | 2.0047(10) |
| Cu(1)-O(1W) | 2.0120(9) |
| Cu(1)-N(2A) | 2.0645(10) |
| Cu(1)-N(2B) | 2.2030(10) |
| | |
| Bond angles | |
| N(1A)-Cu(1)-N(1B) | 169.07(4) |
| N(1A)-Cu(1)-O(1W) | 90.09(4) |
| N(1B)-Cu(1)-O(1W) | 81.30(4) |
| N(1A)-Cu(1)-N(2A) | 81.63(4) |
| N(1B)-Cu(1)-N(2A) | 101.29(4) |
| O(1W)-Cu(1)-N(2A) | 143.41(4) |
| N(1A)-Cu(1)-N(2B) | 109.99(4) |
| N(1B)-Cu(1)-N(2B) | 79.50(4) |
| O(1W)-Cu(1)-N(2B) | 110.14(4) |
| N(2A)-Cu(1)-N(2B) | 106.17(4) |

| Compound 3 | |
|---|---|
| t5=0.82 | |
| Bond length (Angstroms | |
| Cu(1)-N(1)#1 | 1.9902(13) |
| Cu(1)-N(1) | 1.9902(13) |
| Cu(1)-N(7) | 2.1407(14) |
| Cu(1)-N(7)#1 | 2.1408(14) |
| Cu(1)-Cl(1) | 2.3449(6) |
| | |
| Bond angles | |
| N(1)#1-Cu(1)-N(1) | 176.14(8) |
| N(1)#1-Cu(1)-N(7) | 102.50(5) |
| N(1)-Cu(1)-N(7) | 79.87(5) |
| N(1)#1-Cu(1)-N(7)#1 | 79.87(5) |
| N(1)-Cu(1)-N(7)#1 | 102.50(5) |
| N(7)-Cu(1)-N(7)#1 | 105.91(7) |
| N(1)#1-Cu(1)-Cl(1) | 88.07(4) |
| N(1)-Cu(1)-Cl(1) | 88.07(4) |
| N(7)-Cu(1)-Cl(1) | 127.04(4) |
| N(7)#1-Cu(1)-Cl(1) | 127.04(4) |

| Compound 2 | |
|---|---|
| | |
| Bond length (Angstroms) | |
| Cu1-O1N | 2.453 |
| Cu1-N1 | 1.951 |
| Cu1-N2 | 2.065 |
| | |
| Bond angles | |
| N1A-Cu-N2A | 80.67 |
| N1A-Cu-N2B | 101.17 |
| N1-Cu-O1 | 85.11 |
| N1-Cu-O2 | 90.69 |
| N2A-Cu-N2B | 134.04 |
| N2-Cu-O | 88.95 |
| O1-Cu-O2 | 50.18 |

| Compound 4 | |
|---|---|
| t5=0.33 | |
| Bond length (Angstroms) | |
| Cu(1)-N(1) | 2.0034(9) |
| Cu(1)-N(2) | 2.0334(10) |
| Cu(1)-Cl(2)#1 | 2.2578(3) |
| Cu(1)-Cl(1) | 2.2775(3) |
| Cu(1)-Cl(2) | 2.7036(3) |
| Cl(2)-Cu(1)#1 | 2.2579(3) |
| | |
| Bond angles | |
| N(1)-Cu(1)-N(2) | 80.49(4) |
| N(1)-Cu(1)-Cl(2)#1 | 172.33(3) |
| N(2)-Cu(1)-Cl(2)#1 | 94.66(3) |
| N(1)-Cu(1)-Cl(1) | 93.56(3) |
| N(2)-Cu(1)-Cl(1) | 152.79(3) |
| Cl(2)#1-Cu(1)-Cl(1) | 93.423(11) |
| N(1)-Cu(1)-Cl(2) | 87.04(3) |
| N(2)-Cu(1)-Cl(2) | 97.54(3) |
| Cl(2)#1-Cu(1)-Cl(2) | 87.713(11) |
| Cl(1)-Cu(1)-Cl(2) | 108.718(11) |

### 3.2.1 Geometry analysis of compounds **1-4**

The geometry of coordination complexes is an important field of study, as many chemical properties are related to the angles and bond distances between the metal center and the ligands. For example, crystal field theory states that ligand position causes certain d-orbitals to increase in energy, leading to the absorbance of specific wavelengths of light. Four and five-coordinate metal complexes are often described by the geometry index, a numerical value that helps chemists qualitatively describe of the structure using certain angles in the complex. The geometry index for four-coordinate complexes is denoted $\tau 4$, while $\tau 5$ describes five-coordinate complexes. A geometry index of $\tau 4 = 1$ indicates a tetrahedral geometry, $\tau 4=0.43$ indicates a see-saw geometry, and $\tau 4=0$ indicates a square planar. A geometry index of $\tau 5=1$ indicates a trigonal bipyramidal geometry, while a $\tau 5=0$ indicates a square pyramidal geometry.

Compound 1 is similar in structure to a bis polypyridyl complex with an aqua ligand described by Hathaway et al. Compound 1 has a $\tau 5$ of 0.43 while the reference molecule has a $\tau 5$ of 0.75. Both are heavily distorted from ideal geometries, but the reference molecule is similar to trigonal bypyramidal. Compound 1 has a copper-oxygen bond length of 2.01 angstroms, shorter than the analogous 2.16 angstrom bond on the reference compound. This shorter bond length brings the aqua ligand closer to the bipyridine ligands and could cause more steric hindrance for the axial nitrogens. This could be the cause of the non-ideal bond angle of 169.1°, compared to 174.6° on the reference molecule.

Compound 2 is a unique complex in this experiment, in that it is the only one that can be considered six-coordinate, which would require the denotation of octahedral. The axial atoms have an angle of 175.7°, near the ideal angle of 180°. The other atoms sit in

the transverse plane, nearly perpendicular to the axial atoms. However, the angles between the transverse atoms ranges from about 65° to 134°. These are far from the ideal angle of 90°, challenging the octahedral moniker. The main discrepancy between this complex and typical coordination complexes is the weakly coordinating nitrate ion, which doubly bonds to the copper center through the oxygen atoms. These constraint of being only two bonds away causes these atoms to be very near each other as they bond to copper, resulting in a small O-Cu-O angle of 65°. Both bonds to nitrate have a length of 2.45 angstroms, significantly longer than the typical copper-oxygen bond length of about 2 angstroms. In another polypyridyl complex reported by Inci et al, nitrate bonds differently; one oxygen forms a 2.08 angstrom coordination bond with copper while the other weakly interacts at a distance of 2.68 angstroms. As another point of reference, the oxygen in the water molecule of compound 1 bonds to copper at 2.01 angstroms away. Based on other results, the nitrate ion may not be considered a true ligand, but rather a weakly coordinating counter ion. If this ion is treated as a non-coordinating anion, the complex would have a $\tau 4$ of 0.36, nearly a see-saw geometry.

Compound 3 contains one coordinating chloride and one outer sphere counter ion chloride. This complex has a $\tau 5$ of 0.82, classifying it as distorted trigonal bypyramidal. Interestingly, a five-coordinate bis polypyridyl chloro complex synthesized by Liu et al had a $\tau 5$ of 0.083, almost perfectly square planar. The Cu-Cl bond in both complexes is approximately 2.3 angstroms and all Cu-N bonds in these complexes are approximately 2.0. The difference in structure may have resulted from the reagents used, as the reference molecule was synthesized and crystallized from water, while acetonitrile was used for compound 3. The reference molecule also contains 3 water molecules per complex

molecule. The presence of solvent molecules in the crystal lattice may affect the geometry of the complex.

With a $\tau 5$ of 0.33, compound 4 is a dimer complex with a geometry that is best described as distorted square pyramidal. Two analogous compounds (i.e. dimer of mono polypyridyl complexes involving bridging chlorides) reported by Eichler et al had $\tau 5$ factors of 0.13 and 0.86, so there is clearly a range of possible geometries for this class of dimer complexes. In fact, the results of compound 4 in conjunction with the results of Eichler et al may indicate that increasing the size of the alkyl groups at the 4 or 4' position on bipyridine (or the 2,9 position on phenanthroline) causes the geometry to shift from square pyramidal to trigonal bipyramidal.

### 3.2.2 SRB Assay

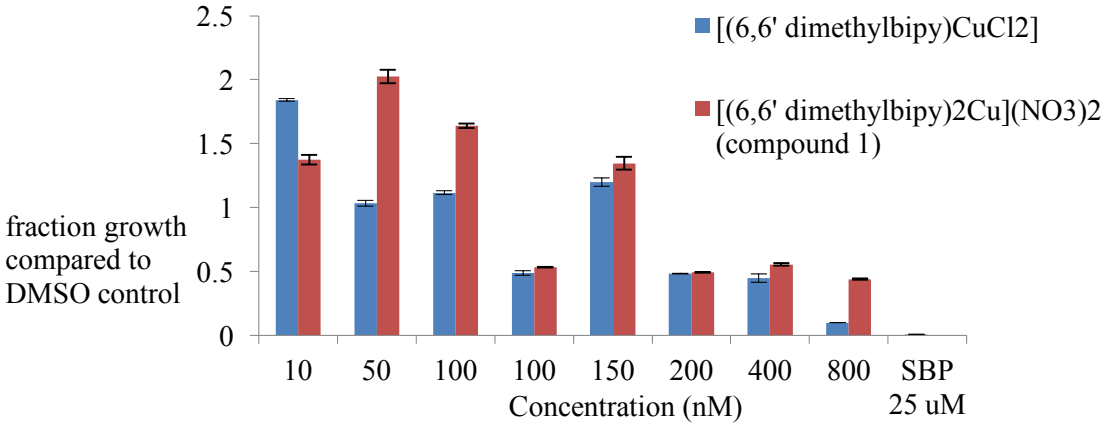


Figure 7.1: Glioblastoma growth versus concentration of mono and bis 6,6' dimethylbipy copper complexes

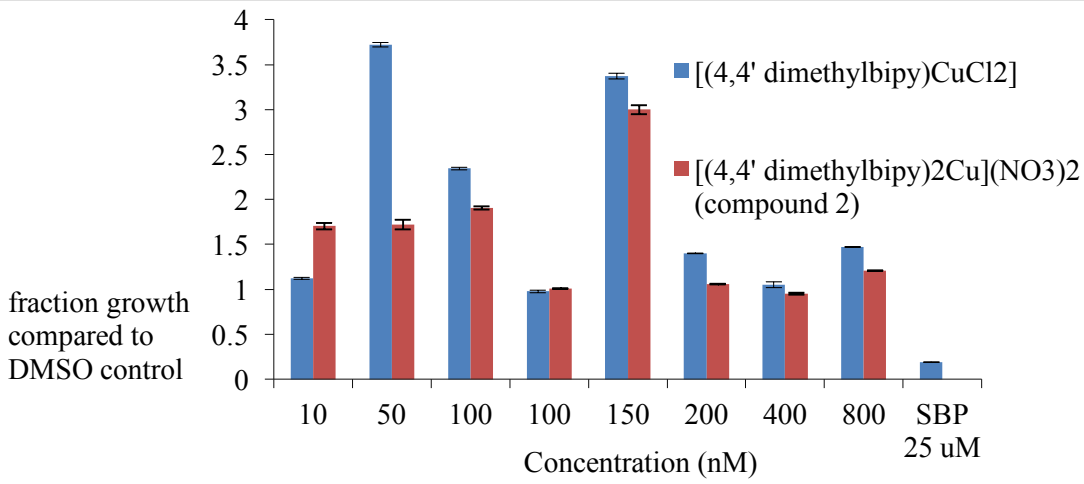


Figure 7.2: Glioblastoma growth versus concentration of mono and bis 4,4' dimethylbipy copper complexes

In order to test a wider range of concentrations, two assays were conducted; one ranged from 10 nM to 150 nM, while the other ranged from 100 nM to 800 nM. Both of these experiments included a concentration of 100 nM, so there are two data points for 100 nM. The data point on the left corresponds to the 10-150 nM assay, while the one on the right corresponds to the 100-800 nM assay.

Linear regression analysis showed that both mono and bis 6,6' complexes inhibited cell growth with increased drug concentration. For the 4,4' complexes, it appears that the mono and bis complexes have negligible activity, as both are at approximately 100% growth at high concentrations. Both complexes will need to be tested at higher concentrations to determine if there is a difference between the two. Several of the smaller concentrations of complexes resulted in a cell growth fraction that was greater than 1. This is most likely due to experimental error in the SRB assay when the drugs are dissolved in dimethyl sulfoxide (DMSO) and added to the cells. In our assay, it is possible that less DMSO was added to the sample wells than to the negative control, resulting in more growth in the samples than in the control. Alternatively, the strange result may indicate that adding drug actually stimulated cell growth. Since cancer cells naturally acquire copper and need it as a cofactor to grow, adding copper drugs in low concentrations could stimulate angiogenesis[17]. At a high enough concentration, the cytotoxic effects of the drug may become strong enough to inhibit the cell growth. The dual potential of copper complexes as both growth factors and cytotoxins is understood and predicted by other researchers[15]. Future work may focus on changing concentrations and determining the concentrations that optimize and minimize cell inhibition.

The SRB assay data suggests an increase in cytotoxicity with the 4,4' bipy bis complex compared to the 4,4' bipy mono complex. The reverse is true for 6,6' bipy bis complexes; There is decreased cytotoxicity with the 6,6' bipy bis complex compared to the 6,6' bipy mono complex. Although these trends are consistent, they are not substantial enough to warrant a conclusion that either bis or mono complexes are more cytotoxic to glioblastoma cells.

There are many factors that may have influenced this. First, the exact type of cancer may change the results. To fairly compare my results to others who have reported increased cytotoxicity in bis complexes[19], the cells tested should be identical. Another variable in this experiment was the anion that balanced the positive charge of copper (II). X-ray crystal structures showed that compound 1 existed as a positively charged molecule with nitrate counter ions while compound 2 had one nitrate counter ion and another weakly bonded nitrate, which may dissociate in solution. The mono complexes, on the other hand, had two chloride ligands, covalently bonded to the copper atom. It may be more difficult for the charged bis complexes to pass through the hydrophobic lipid bilayer in the cell membrane and nuclear membrane. This could explain why the mono complexes had a higher cytotoxicity, even though bis complexes were predicted to be more effective. An experiment to determine the difference between mono and bis complexes with a consistent anion should be conducted in order to fairly compare the effects of bis and mono complexes. Synthesis of bis complexes with chloride ligands as anions proved difficult, so it may be simpler to synthesize mono complexes with nitrate anions to compare to the reported bis complexes. Mono complexes that contain nitrate anions should be synthesized and tested in an SRB assay to determine the difference in cytotoxicity based purely on the number of ligands.

Differences in structure and may have also affected how each one interacted with DNA. Given that the 4,4' complexes had much less cytotoxic activity than the 6,6' complexes, I hypothesize that placement of methyl groups on the polypyridyl ligand may play an important role in the activity of the drug. The methyl groups could conceivably block intercalation with the minor groove of the DNA, preventing cleavage. Placement of

methyl groups may also affect the redox activity of copper. Based on the results of this experiment, I predict that 4,4' bipy prevents copper (II) from catalyzing DNA oxidation. These potential mechanisms deserve further study. Cyclic voltammetry may be used to further study the reduction potentials of these complexes. I predict that the complexes that effectively inhibited cell growth have higher reduction potentials, as this would allow them to better oxidize DNA.

## 4. Conclusion

I successfully synthesized four novel copper complexes. X-ray crystallography showed that three of the compounds were bis complexes, and one was a dimer of mono complexes. Although two of the compounds had questionable purity (the elemental analysis did not support the x-ray crystal structure), the other two had structures that were supported by elemental analysis, indicating purity. To summarize the synthesis results, starting materials with nitrate anions were more likely to form pure bis complexes than starting materials with chloride anions.

My hypothesis that bis complexes would be more cytotoxic than mono complexes was shown to be true for complexes with 4,4' bipy, but false for complexes with 6,6' bipy in this experiment. This may be due to the geometries and sterics of the complexes, as cytotoxicity is related to the ability of the complex to effectively bind to DNA. To determine the DNA binding constants, a UV-vis spectroscopy experiment should be conducted.

The dual potential of copper complexes as growth cofactors and cytotoxins is revealed in the SRB analysis. At low concentrations, the drug stimulates cell growth, while it inhibits growth at higher concentrations. This property of copper complexes is predicted

by Santini et al. The SRB assay gives interesting insight into the role that the counter ion may play in inhibiting cell growth; chloride as the anion may increase cytotoxicity. To test this observation, an SRB assay using the [bis 6,6' dimethylbipy $CuCl_2$] complex should be conducted and compared to the results of the [bis 6,6' dimethylbipy $Cu(NO_3)_2$] complex from this experiment. Additional future work may involve determining the redox properties of these complexes and testing the cytotoxicity of these compounds with other kinds cancer cells.

Glioblastoma, an uncured disease with 100,000 new cases each year, is a deadly threat to humanity. Researchers continue to learn more about this cancer and elucidate its biochemical pathways. Although there is no cure yet, copper complexes are a candidate to treat this disease. Compounds that include this naturally occurring metal have the potential for selectivity, low dosage, and reduced side effects, all of which are major advantages over platinum based chemotherapeutics. The proposed mechanism of copper complexes, DNA binding and cleavage, may give it an advantage over Temozolomide, which can be countered by DNA repair proteins. Although the reported compounds did not inhibit cancer growth as well as I predicted, this study showed several important properties of copper drugs and asks new questions that will drive research.

Works Cited

1. Quinn T. Ostrom, L. B., Faith G. Davis, Isabelle Deltour, James L. Fisher, Chelsea Eastman Langer,; Melike Pekmezci, J. A. S., Michelle C. Turner, Kyle M. Walsh, Margaret R. Wrensch,; Barnholtz-Sloan, a. J. S., The epidemiology of glioma in adults: a "state of the science" review. *Neuro-Oncology* **2014,** *16* (7), 896-913.

2. Minniti, G.; Muni, R.; Lanzetta, G.; Marchetti, P.; Enrici, R. M., Chemotherapy for glioblastoma: current treatment and future perspectives for cytotoxic and targeted agents. *Anticancer Res* **2009,** *29* (12), 5171-84.

3. Burger PC, H. E., Shibata T, Kleihues P, Topographic anatomy and CT correlations in the untreated glioblastoma multiforme. *Journal of Neurosurgery* **1988,** *68* (5), 698-704.

4. Glioblastoma (GBM). American Brain Tumor Association.

5. Gallego, O., Nonsurgical treatment of recurrent glioblastoma. *Current Oncology* **2015,** *22* (4), e273-e281.

6. Hegi ME, D. A., Gorlia T, et al, MGMT gene silencing and benefit from temozolomide in glioblastoma. *N Engl J Med* **2005,** *352*, 997-1003.

7. Auranofin for the treatment of rheumatoid arthritis. National Library of Medicine, National Institutes of Health: PubMed Health, 2008.

8. Büsselberg, A.-M. F. a. D., Cisplatin as an Anti-Tumor Drug: Cellular Mechanisms of Activity, Drug Resistance and Induced Side Effects. *Cancers* **2011,** (3), 1355.

9. Amr Amin, M. A. B., New Platinum and Ruthenium Complexes - the Latest Class of Potential Chemotherapeutic Drugs - a Review of Recent Developments in the Field. *Mini-Reviews in Medicinal Chemistry* **2009,** *9*, 1489-1503.

10. Wong, E.; Giandomenico, C. M., Current status of platinum-based antitumor drugs. *Chem Rev* **1999,** *99* (9), 2451-66.

11. RM Baldwin, M. G.-L., DAE Parolin, PM Krzyzanowski, MA Andrade, and; Lorimer, I., Protection of glioblastoma cells from cisplatin cytotoxicity via protein kinase Ci-mediated attenuation of p38 MAP kinase signaling. *Oncogene* **2006,** *25*, 2909-2919.

12. Emmanuel S. Antonarakis, A. E., Ruthenium-based chemotherapeutics: are they ready for prime time? *Cancer Chemother Pharmacol* **2010,** *66*, 1-9.

13. Pauline M. Olsen, C. R., Daniel Lussier, Brian Khoa Le, Noah Angel, Michelle Smith, Chihyun (Brian) Hwang, Raneen Khatib, Julia Jenkins, Kaitlyn Adams, Jonathan Getcher, Fook Tham, Zhou (Georgia) Chen, Emma H. Wilson, Jack F. Eichler, Synthesis, characterization, and antitumor activity of unusual pseudo five coordinate gold(III) complexes: Distinct cytotoxic mechanism or expensive ligand delivery systems? *Journal of Inorganic Biochemistry* **2014,** *141*, 121-131.

14. Dou, V. M. a. Q. P., The tumor proteasome as a novel target for gold(III) complexes: implications for breast cancer therapy. *Coord Chem Rev* **2009,** *253* (11-12), 1649-1660.

15. Carlo Santini, M. P., Valentina Gandin, Marina Porchia, Francesco Tisato, and Cristina Marzano, Advances in Copper Complexes as Anticancer Agents. *Chemical Reviews* **2014,** *114*, 815-862.

16. Q3D Elemental Impurities: Guidance for Industry. Services, U. S. D. o. H. a. H., Ed. 2015.

17. Xie, H.; Kang, Y. J., Role of copper in angiogenesis and its medicinal implications. *Curr Med Chem* **2009,** *16* (10), 1304-14.

18. Tiziana Pivetta, F. T., Elisa Valletta, Francesco Isaia, Carlo Castellano, Francesco Demartin, Rossana Tuveri, Sarah Vascellari, Alessandra Pani, Novel copper(II) complexes as new promising antitumour agents. A crystal structure of [Cu(1,10-phenanthroline-5,6-dione)2(OH2)(OClO3)](ClO4). *Journal of Inorganic Biochemistry* **2014,** *141*, 103–113.

19. Duygu Inci, R. A., Dilek Yılmaz, Hasene Mutlu Gençkal, Özgür Vatan, Nilüfer Çinkılıç, Yunus Zorlu, New water-soluble copper (II) complexes including 4,7-dimethyl-1,10-phenanthroline and L-tyrosine: Synthesis, characterization, DNA interactions and cytotoxicities. *Spectrochimica Acta Part A: Molecular and Biomolecular Spectroscopy* **2015,** *136*, 761-770.

20. Harris, D. C., In *Quantitative Chemical Analysis*, 8 ed.; W. H. Freeman and Company: New York, NY, 2010; pp 682-685.

21. P. Skehan, R. S., D. Scudiero, A. Monks, J. McMahon, D. Vistica, J.T. Warren, H.; Bokesch, S. K., M.R. Boyd, *J. Natl. Cancer Inst.* **1990,** *82*, 107-112.

22. J.Hathaway, W. D. H.-B., The crystal structure of monoaquabis(2,2'-bipyridyl)copper(II) dithionate. *Acta Crystallographica Section B Structural Crystallography and Crystal Chemistry* **1979,** *B35*, 2910-2913.

23. Liu He, L. C., Zhong Bohua, Synthesis and crystal structure of [Cu(II)(bipy)2Cl]·NO3·3H2O. *Chemical Journal on Internet* **2004,** *6* (7), 1523-1623.

24. *APEX 2,* version 2014.1-1, Bruker (2014), Bruker AXS Inc., Madison, Wisconsin, USA.

25. *SAINT,* version V8.34A, Bruker (2012), Bruker AXS Inc., Madison, Wisconsin, USA.

26. *SADABS,* version 2012/1, Bruker (2012), Bruker AXS Inc., Madison, Wisconsin, USA.

27. *SHELXTL,* version 2013/4, Bruker (2013), Bruker AXS Inc., Madison, Wisconsin, USA.